# Coordinated assembly and release of adhesions builds apical junctional belts during *de novo* polarisation of an epithelial tube

Andrew C Symonds[*2], Clare E Buckley[*1,2, 3], Charlotte A Williams[2] & Jonathan DW Clarke[1,2]

* Equal contribution
1. Corresponding authors

2. Centre for Developmental Neurobiology,
Institute of Psychiatry, Psychology and Neuroscience
King's College London
Guy's Campus
London
SE1 1UL

3. Department of Physiology, Development and Neuroscience
University of Cambridge
Downing Street
Cambridge
CB2 3BY

**Abstract**

Using the zebrafish neural tube as a model, we uncover the *in vivo* mechanisms allowing the generation of two opposing apical epithelial surfaces within the centre of an initially unpolarised, solid organ. We show that NOK/Pals1/Mpp5a and Rab11a play a dual role in coordinating the generation of ipsilateral junctional belts whilst simultaneously releasing contralateral adhesions across the centre of the tissue. We show that Nok and Rab11a mediated resolution of cell-cell adhesions are both necessary for midline lumen opening and contribute to later maintenance of epithelial organisation. We propose these roles for both Nok and Rab11a operate through the transmembrane protein Crumbs. In light of a recent conflicting publication, we also clarify the junction remodelling role of Nok is not specific to dividing cells but remodelling during cell division aligns both ipsilateral and contralateral junctions more closely to the midline of the tissue.

## Introduction

Epithelia are one of the fundamental tissue types of the body, forming protective sheets of cells around the outside of the organism and lining the inside surface of many organs or parts of organs. All epithelia are polarised and have an apical and a basal surface that are molecularly and functionally distinct. In some cases, the organisation of the apical surface of an epithelium is generated at the free surface of an embryonic sheet of cells while in others the apical surface emerges from within a dense rod or ball of cells to generate an epithelial tube or cyst. Generating an apical surface from within a rod or ball of cells adds an extra layer of complexity to this process as cells at the centre of these structures have to lose inappropriate connections to generate a free surface as well as organising that free surface into a typical apical structure comprising a lattice of closely adherent cells connected by apicolateral belts of specialised junctions (typically adherens junctions and tight junctions in vertebrates). To what extent similar mechanisms of apical surface development are employed at a free surface compared to within a rod or sphere primordium, and how these can be coordinated with the remodelling of cell-cell connections necessary for *de novo* surface generation, is poorly understood, especially *in vivo*.

Here we analyse the spatial deployment of the cardinal polarity protein Pard3 and the cell adhesion protein Cdh2 during generation of the apical surface of the neural tube in the zebrafish embryo *in vivo*. In this system the apical surface is generated *de novo* from within the solid neural rod and the relative accessibility and transparency of the zebrafish embryo provides an advantageous system in which to address mechanism in whole embryos. We use experimental manipulations of the NOK/Pals1/Mpp5a scaffold protein and the endocytic recycling protein Rab11a to determine the cellular and molecular mechanisms that simultaneously remodel cell-cell connections in order to release cell adhesions across the organ midline and generate the canonical apical junctional belt organisation of epithelia within a solid primordium. We compare these to previously shown mechanisms that generate apical organisation at a free surface (Grawe et al., 1996, Harris & Peifer, 2005, Morais-de-Sa et al., 2010, Tepass, 1996). Our results show that both Mpp5a and Rab11a are required to remodel connections between contralateral and ipsilateral cells and we suggest they operate through apical recruitment of the transmembrane protein Crumbs.

## Results

### Apical rings of Pard3 and ZO-1 are built up from the ventral floor plate

The apical surface of epithelia is characterised by a lattice-like arrangement of polarity and scaffolding proteins (such as Pard3, aPKC, ZO-1) and cell adhesion proteins (such as Cdh2). We visualised this organisation prior to lumen opening in the sagittal plane of the developing zebrafish neural rod (stages 10 to 18 somites, 14 to 18 hpf) at the level of the nascent anterior spinal cord (Figure 1A, B).We generated a BAC transgenic fish line that reports the endogenous spatiotemporal expression of Pard3, a cardinal polarity protein, in live embryos and by using an antibody for the MAGUK (membrane association and presence of the GUK domain) scaffolding molecule ZO-1 (also known as tight junction protein) on fixed tissue.

At early neural rod stages (11 somite-stage), we saw that apical rings of Pard3-EGFP and ZO-1 were first established at the midline in ventral floor plate cells (Figure 1B, e.g. arrows). In more dorsal areas of the neuroepithelium, where apical rings had not yet formed, Pard3-EGFP and ZO-1 were seen as puncta (Figure 1B, e.g. arrowheads), reminiscent of spot adherens junctions in other systems (e.g. Tepass et al., 1996). Over the next few hours of rod stage (up to 17 somite-stage) the lattice work of apical rings progressively builds from ventral to dorsal such that at any given timepoint there is a developmental gradient along the dorso-ventral axis of the nascent neuroepithelium (Figure 1B). In contrast to a previous study (Guo et al., 2018) our results suggest Pard3 is an early component of the nascent apical junction organisation, with both Pard3 and ZO-1 expressed in a punctate manner during a very dynamic phase of cell interdigitation across the neural keel midline (current results and Buckley et al., 2013)

### Pard3 puncta initially appear at multi-cellular junctions

To gain a better understanding of where in the cell Pard3 puncta first appear, we labelled Pard3-EGFP embryos with membrane-tagged mNeptune2.5 and imaged at neural keel stage prior to apical surface formation. We found Pard3-EGFP puncta were seen close to the midline around the perimeter of the cells, often at multi-cellular interfaces (vertices where more than two cells meet (Figure 1C, e.g. arrowheads). Membrane tagged mNeptune was not enriched at these multi-cellular interfaces indicating the Pard3-EGFP enrichment is not simply due to more membrane at these points. This is consistent with Pard3 puncta being located at the nascent apical cortex of the cell. The later ring-like domains of Pard3 appear to be built by Pard3 puncta subsequently being added at cell-cell interfaces between the TCJs until they coalesce to form a more or less continuous ring structure (Figure 1D).

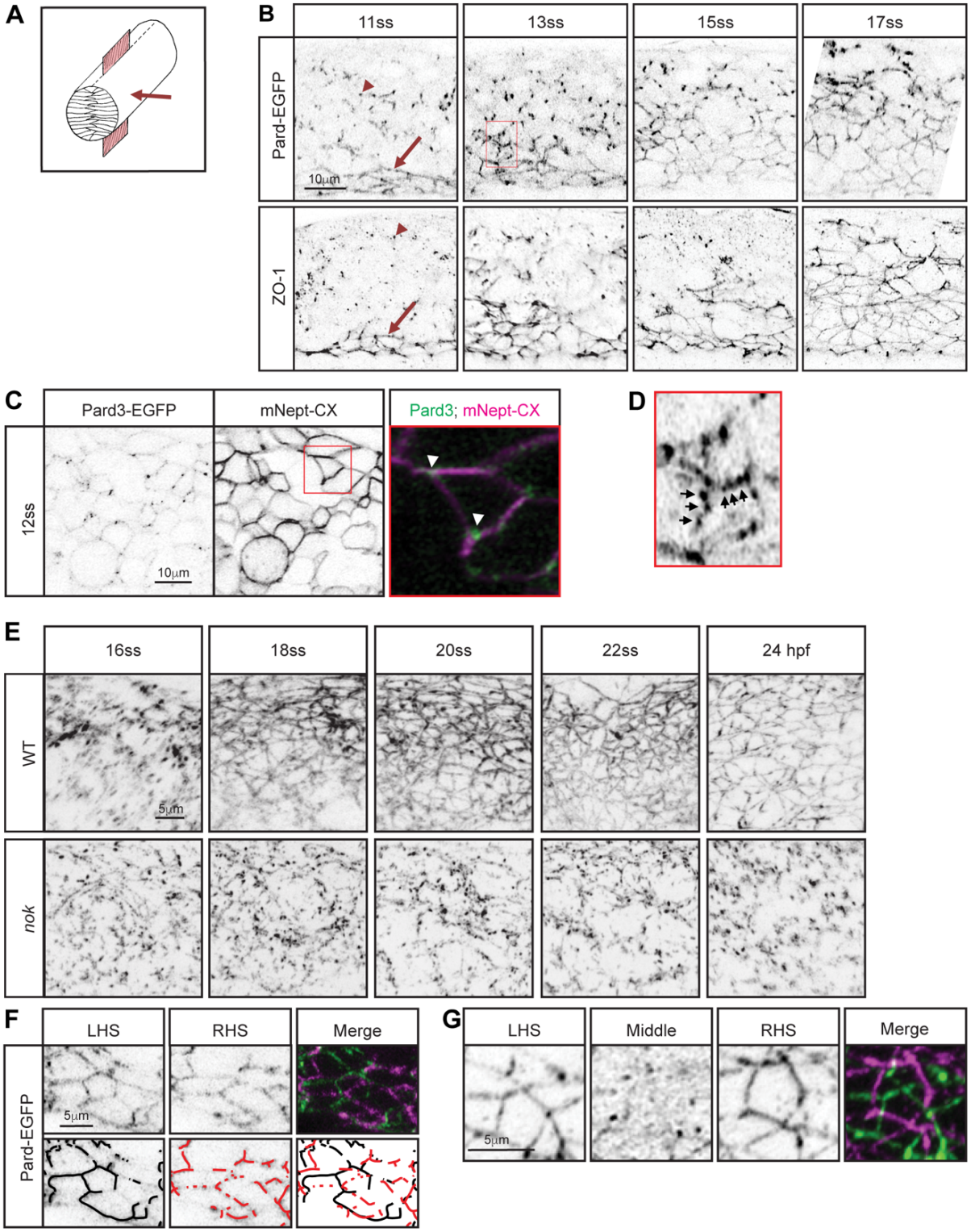


**Figure 1. Nok dependent spot adhesion to apical ring transition.**

**A)** Diagram of neural rod with inserted red sheet to illustrate sagittal plane of confocal optical sections. Red arrow indicates direction of imaging.
**B)** Sagittal confocal planes of neural rod in anterior spinal cord region at 11, 13 , 15 and 17 somite stages. Top row shows expression of Pard3-EGFP. Bottom row shows expression of ZO-1. Red arrow indicates ventral apical rings. Dorsal to top.

**C)** Sagittal confocal images at 12 somite stage showing Pard3-EGFP puncta are often located at multi-cellular junctions (arrowed). Plasma membrane imaged using mNeptune-CAAX (mNept-CX).
**D)** Enlarged area outlined in red in B to show nascent apical rings appear to be formed from multiple Pard3-EGFP puncta.
**E)** Time series of sagittal confocal sections from wildtype and *nok* mutant neural rods showing *nok* mutants never progress from punctate Pard3-EGFP to apical ring formation.
**F)** Parasagittal confocal sections from left hand side (LHS) and right-hand side (RHS) of stage 15somite neural rod. Incomplete apical rings of Pard3-EGFP are forming independently on left and right sides of the midline.
**G**) Parasagittal and sagittal confocal sections at 17 somite stage showing complete apical rings of Pard3-EGFP on either side of the midline. The sagittal section (labelled Middle) shows a largely diffuse low level of Pard3-EGFP expression in the midline territory between the left and right rings.

## ***nok$^{m227}$*** **mutants fail to undergo puncta to apical ring transition**

To begin to uncover the mechanisms that regulate formation of the apical junctions in the sagittal plane of the neural rod we examined the apical puncta to ring transition in a mutant fish line that fails to open a lumen. Nok/Mpp5a is a MAGUK scaffolding protein (Wei & Malicki, 2002b), essential to retain all forms of the transmembrane protein Crumbs at the apical surface (Zou et al., 2013) and *nok* mutants have previously been reported to fail to generate an open a lumen in the neural rod and to have disorganised adherens junctions (Lowery et al., 2009, Lowery & Sive, 2005). We found that although *nok*$^{m227}$ mutants generate Pard3-EGFP puncta in the sagittal plane at the 16-somite stage, these puncta failed to undergo the puncta-to-apical ring transition and remained as punctate deposits throughout development (Figure 1E). Nok/Mpp5a is thus critical to build apical junctional rings.

## **Apical rings on either side of the tissue midline develop independently and are offset from one another**

To successfully undergo *de novo* lumen formation, the zebrafish must generate not one, but two lattice-like apical surfaces in the middle of a solid tissue, one on the left side and one on the right side of the future lumen. One possibility is that a single plane of apical rings may first develop at the left-right interface and then these pioneer rings might split into left and right rings. To assess this hypothesis, we carefully analysed the development of left and right rings. Imaging sagittal and parasagittal planes we never saw a plane with single apical rings (10 embryos, Figure 1F, G). Instead, apical rings were always found bilaterally, and incomplete apical rings were also found bilaterally on either side of the midline, showing left and right rings are built independently. Furthermore, we observed that the developing rings on either side of the tissue midline are always offset from one another, rather than having a mirror-symmetric arrangement that might be expected if individual rings split into two (Figure 1G).

**Non-sister connections impose cell offsets across the midline**

Most neural rod cells derive from progenitors that divide at the midline to generate mirror-symmetrically polarised sisters connected to each other across the midline (called the C-division) (Buckley et al., 2013, Kimmel et al., 1994, Tawk et al., 2007). This process will at least temporarily align pairs of sister cells across the midline. However, the offset organisation of left and right apical rings suggests a mechanism must exist that adds offset to this initial cell alignment. To confirm that sister cells become offset, we first generated mosaically labelled embryos and used live imaging to assess the development of the midline interface between sister cells. Soon after a midline mitosis, sister cells were mirror-symmetric to each other across the tissue midline (Figure 2A, 13 somites). However, following the C-division the interface between sister cells was highly dynamic. Both the shape and the location of the sister interface changed over time (Figure 2A up until 35 minutes). By the neural rod stage, the connection between the sisters was stably offset such that the nascent apical endfeet met at their corners (Figure 2A, 18 somites). These observations show that an initially rather good mirror-symmetric sister cell alignment is shifted to an offset organisation following C-division mitosis. The offset conformation between C-division sister cells suggests that cell connections across the midline might not be confined to their C-division sisters.

Additionally, by imaging dividing cells and their neighbours, we were also able to infer that the offset between C-division sisters is initiated during C-division mitosis itself and acts to locally align junctions between sister and non-sister cells. To examine the dynamics of ipsilateral and contralateral cell adhesions during the process of the midline C-division, we took advantage of a BAC transgenic line expressing the cell adhesion protein Cdh2 fused to a tandem fluorescent timer (Revenu et al., 2014) and we imaged Cdh2-GFP from this line. Cdh2-GFP is expressed in all neural rod cells over the entire plasma membrane. Prior to C-divisions, cells intercalate across the rod midline and Cdh2-GFP is enriched in this interdigitation zone, showing that cells contact and adhere to several contralateral cells (Figure 2Bi). When cells enter mitosis at or close to the midline, distinct enrichments of Cdh2-GFP became largely localised to the cleavage furrow between sister cells during telophase (red arrows, Figure 2Bi). During cleavage furrow ingression, we found that cell processes from neighbouring cells moved into the cleavage furrow, pulling both ipsilateral and contralateral cell contacts into a narrower mediolateral plane. Throughout this process, the mitotic cells remain connected to multiple contralateral partners. As cartooned in Figure 2Biii, this mechanism draws multiple local Cdh2 connections into a plane that is more precisely aligned to the tissue midline, while the maintenance of several contralateral contacts through mitosis contributes to an offset between C-division sisters. By the neural rod stage, the left-right interfaces between cells is aligned precisely to the midline, with Cdh2-GFP enrichments often localised to their apical

corners (Figure 2Bii, arrowheads). To see if this offset cell conformation persists until lumen opening, we looked at electron micrographs taken at the very start of lumen inflation. This showed a striking zig-zag conformation between cells separating across the apical midline (Figure 2C). It therefore appears that the offset conformation between left and right cells persists until the lumen inflates, separating the left and right sides of the neural rod.

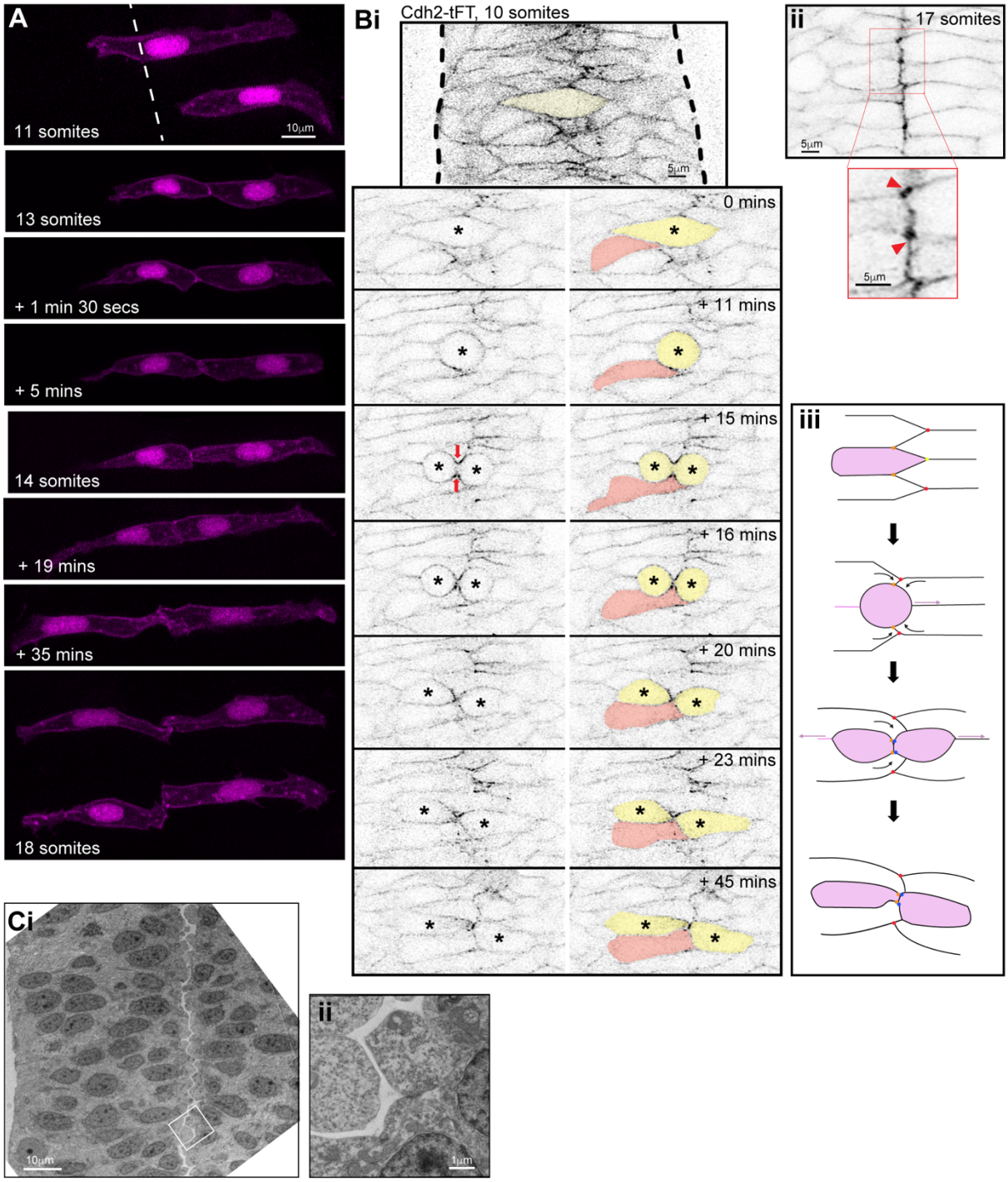


**Figure 2. Sister-cells remain attached via their corners**
**A)** Images from a time-lapse movie projection in dorsal orientation of mosaically labelled neuroepithelial cells in the hindbrain of an 11-somite stage WT embryo from neural keel stage. Membrane and nuclei are labelled in magenta. By the 13-somite stage, both cells had undergone C-division, resulting in pairs

of sister cells attached across the tissue midline. The top cell pair was followed over time until the 18-somite neural rod stage, when both cell pairs were imaged. The shape and location of the connection point between sister cells dynamically altered over the neural keel to rod transition. However, by the neural rod stage, the connections between both pairs of cells were markedly offset and cells remained connected contralaterally via their apical corners. The configuration of cell pair connections was assessed from several different experiments at the neural rod stage (approximately 16-18 somites) and 26/31 pairs of cells from 5 embryos at neural rod stages were found to be clearly attached via their corners. The remaining 5 were either connected via a more 'en face' configuration or their configuration was uncertain (e.g. due to a very thin connection point).
**B) i.** Single z-planes from a time-lapse movie of a C-division starting at the 10-somite stage (neural keel) from a Cdh2-tFT transgenic embryo. Cdh2-GFP becomes strongly concentrated in the cleavage furrow and neighbouring cells ingress into the cleavage furrow (21/21 divisions, red arrows). As the dividing cells reintegrate into the epithelium the interface with neighbouring cells becomes straighter around the midline. Dividing cell is highlighted in yellow and ingressing neighbouring cell in red.
**ii.** 5μm projection of 17-somite stage neural rod from a Cdh2-tFT transgenic embryo. Cells are well aligned along a centrally located midline. Cdh2-GFP is upregulated along the apical midline, particularly at cell corners where Cdh2-GFP enrichments can often be seen in pairs (red arrowheads in magnified region).
**iii.** Diagram depicting an example of the co-ingression of neighbouring cells into the cleavage furrow during C-division. Adhesions between cells are represented by coloured dots.
**C) i.** Transmission electron micrographs of a 20 h.p.f. embryo hindbrain in transverse orientation. The lumen has just started to open from the midline. The interface between contralateral cells has a striking 'zig-zag' pattern. **ii.** Magnified region from **i**.

## A single midline interface enriched in polarity and cell adhesion proteins precedes the formation of bilateral apical rings

To better understand the transition from spot-like junctional specialisations to two independent lattices of apical rings on left and right sides of the neural rod midline we analysed the distribution of Pard3 and the adhesion protein Cdh2 during this transition. Since there is a developmental gradient along the dorso-ventral axis of the neuroepithelium (Figure 1B), we focused on a mid-dorsoventral plane of the anterior spinal cord. We imaged Pard3-EGFP and Cdh2-GFP from neural keel through to neural rod stages in the horizontal plane (Figure 3Ai). This showed that Pard3-EGFP and Cdh2-GFP initially have different temporal patterns of expression. At the 11-somite stage (14 h.p.f., neural keel stage) Pard3-EGFP was localised broadly in the interdigitation zone around the tissue midline in short, discontinuous mediolaterally oriented stripes. These stripes where composed of puncta of Pard3-EGFP and correspond to the spot distribution of Pard3-EGFP seen in sagittal sections (Figure 1B). At the same timepoint Cdh2-GFP was expressed at low level throughout the cell membrane but also slightly elevated in the interdigitation zone, mostly in discrete spots. By the 17-somite stage (17.5 h.p.f., neural rod stage), both Cdh2-GFP and Pard3-EGFP were clearly enriched at the midline in a near continuous, fairly straight expression domain at the interface between left and right cells. Consistent with a developmental gradient along the dorso-ventral axis of the neuroepithelium, dorsal to this plane, Cdh2-GFP and Pard3-EGFP were still expressed in a discontinuous mediolateral stripe pattern, and ventral to this plane these proteins appeared in two parasagittal domains either side of the tissue midline (Figure 3Aii). The intermediate level that shows a single left-right interface of Pard3-EGFP and Cdh2-GFP expression occupies

only a small and transient dorsoventral domain that progresses dorsally as the assembly of bilateral rings progresses from ventral to dorsal.

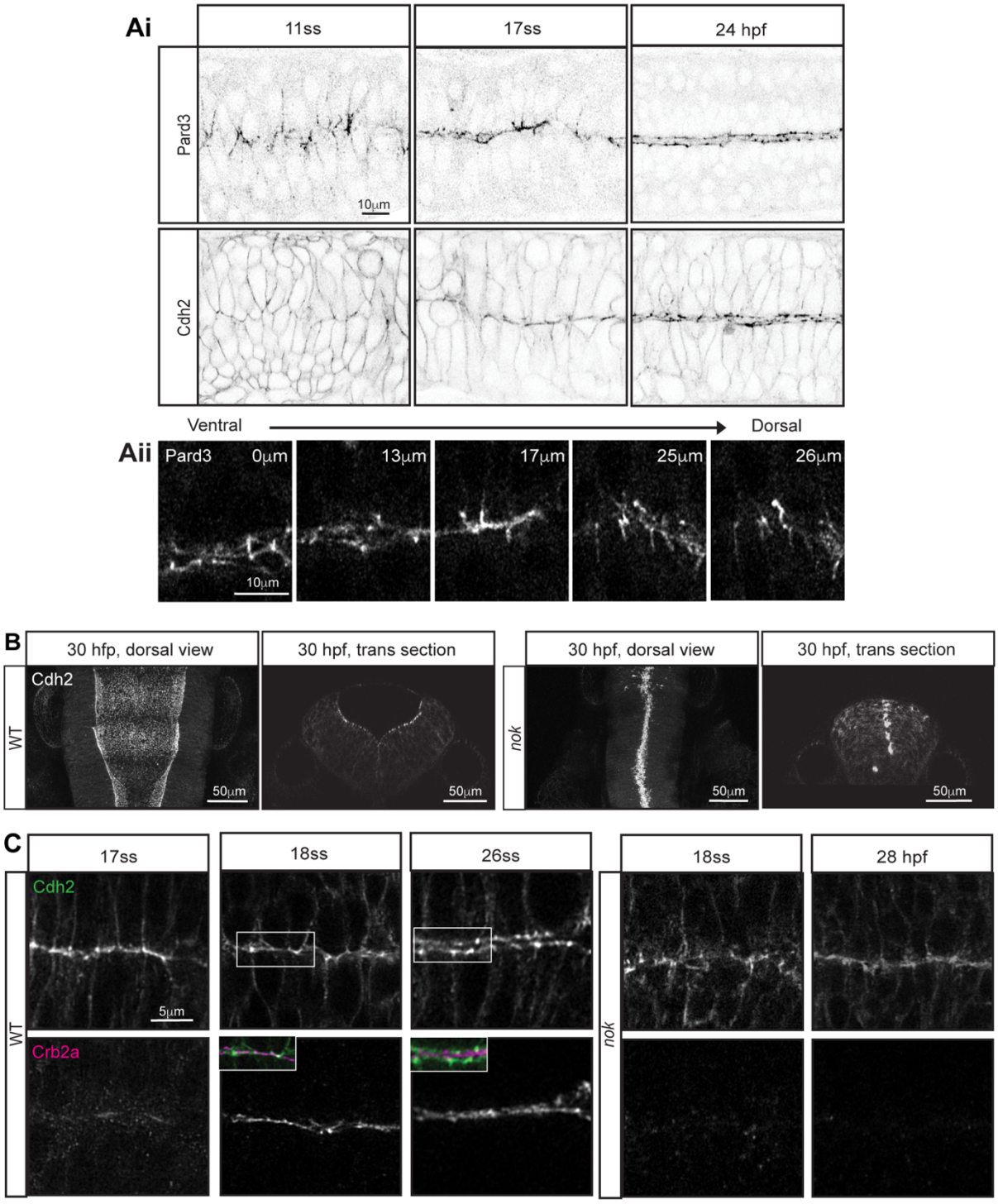


**Figure 3. Nok dependent remodelling of midline adhesions.**
**Ai)** Horizontal confocal planes of neural rod in anterior spinal cord region at 11 somite, 17 somite and 24 h.p.f. stages. Top row shows expression of Pard3-EGFP. Bottom row shows expression of Cdh2-GFP.
**Aii)** Horizontal confocal planes of 17 somite stage neural rod showing Pard3-EGFP expression at five different dorsoventral levels. The single elevated plane of expression at the left right interface seen at

level 17 µm lies dorsal to levels where apical rings are already formed and ventral to levels where expression is more prominent in mediolateral streaks.
**B)** Horizontal and transverse confocal sections at hindbrain level of 30 h.p.f wildtype and *nok* mutant embryos. Apical surface of neuroepithelium revealed by Cdh2-GFP.
**C)** Horizontal confocal sections at anterior spinal cord level in wildtype and *nok* mutant embryos imaged for Cdh2-GFP and Crb2a immunoreactivity. Crb2a is not present in the sagittal plane in *nok* mutants and the independent rings of Cdh2-GFP on left and right sides of the midline do not form in *nok* mutants. Insets in the 18 and 26 somite stages of wildtypes show merge of Crb2a and Cdh2-GFP expression.

By 24 h.p.f, although spinal cord cells at almost all dorsoventral levels do still meet at the left-right interface, Pard3-EGFP and Cdh2-GFP no longer localise to this interface; rather their expression has fully transitioned from mediolaterally arranged puncta through a single midline expression domain and into two parasagittal domains either side of the tissue midline (Figure 3Ai). These two domains are characterised by periodically elevated spots of expression that correspond to points within the left and right apical rings. Much lower levels of both Pard3-EGFP and Cdh2-GFP remain in the medial zone between the bilateral apical rings.

These data suggest left and right cells initially adhere together across the midline through Cdh2-rich adhesions, but this interface is then largely cleared of both Cdh2 and Pard3 as these adhesion and polarity proteins are redeployed more basally to the apicolateral border where they contribute to adhesive junctions between ipsilateral cells. This basolateral redeployment of junctional proteins is likely to be a critical step in the process of releasing cells from their contralateral adhesions that allows lumen formation.

**Nok/Mpp5a is required to remodel adhesions across the midline**

Work in *Drosophila* epithelia has shown that Crumbs is required for the proper localisation of Baz (*Drosophila* Pard3) and E-cadherin at apical junctions, displacing them from the apical-most surface of single sheet epithelial cells to the apico-lateral border of the cell (Grawe et al., 1996, Harris & Peifer, 2005, Morais-de-Sa et al., 2010, Tepass, 1996). Although eliminating Crumbs in zebrafish is difficult because there are multiple Crumbs proteins, we took advantage of the *nok*$^{m227}$ mutant that is unable to localise Crumbs proteins to the apical surface (Zou et al., 2013). Since we earlier demonstrated that the apical spot to ring transition did not occur in *nok*$^{m227}$ mutants (Figure 1E), we next wanted to test the role for Nok in displacing Pard3 and Cdh2 proteins from a single line at the left-right interface, to the two bilateral expression domains seen at more mature time points. To do this we generated a *nok*$^{m227}$ mutant; Cdh2-tFT compound transgenic line. Whereas 'wild-type' Cdh2-tFT embryos opened a lumen in hindbrain and anterior spinal cord (Figure 3Bi), *nok*$^{m227}$; Cdh2-tFT embryos failed to open a lumen (Figure 3Bii), in line with previous observations on *nok* (Lowery & Sive, 2005).

To understand the *nok*$^{m227}$ phenotype in relation to Cdh2 remodelling and its relation to Crumbs expression, we examined the localisation of both proteins in wild-type and *nok*$^{m227}$ embryos. In wild-type embryos (Figure 3C) Crumbs2a is first expressed at the neural rod 17/18 somite stage at the left-right interface, coincident with a single line of expression of Cdh2. However, by the 26-somite stage, when Crumbs2a protein was still localised to the left-right interface, Cdh2-GFP protein was displaced to form two slightly more basolateral lines of expression. The Cdh2-GFP expression was located immediately lateral to Crumbs2a, with very little overlap of expression.

In *nok*$^{m227}$ mutant embryos (Figure 3D) Crumbs2a expression is absent from the midline as expected. At the neural rod 18 somite stage *nok*$^{m227}$ mutant Cdh2-tFT embryos showed a single domain of enrichment of Cdh2-GFP at the left-right interface similar to wild-type Cdh2-GFP embryos. However, unlike wild-type embryos, Cdh2-GFP expression remained as a single midline domain in *nok*$^{m227}$ mutants and failed to undergo the transition to two lines of Cdh2-GFP either side of the tissue midline, even up to stages as late at 28 h.p.f.

Together, these data show that left and right cells initially adhere together across the midline through contralateral adhesions. However, both Cdh2 and Pard3 adhesion and polarity proteins are then redeployed more basally to the apicolateral border where they contribute to adhesive junctions between ipsilateral cells to build coherent, bilateral sheets of neuroepithelial cells. This basolateral redeployment of junctional proteins depends on Nok/Mpp5a, presumably through its ability to localise Crumbs proteins to the left-right interface and is likely to be a critical step in the process of releasing cells from their contralateral adhesions to allow lumen formation at more anterior regions of the neural tube. The lack of basal displacement of junctional proteins in *nok*$^{m227}$ mutants allows the persistent adhesion between cells on left and right sides and this is likely to cause the inhibition of lumen formation.

**Persistent adhesions may contribute to lack of epithelial maintenance in Nok and Rab11a deficient epithelia**

To test the hypothesis that Nok deficient cells retain persistent adhesions across the midline, we analysed the behaviour of clonally related cells in the hindbrain regions of 25 h.p.f. wild type embryos that had open lumens and *nok* morphant embryos that were unable to open a lumen. In wild type embryos, cells had successfully separated across the midline following C-division; they maintained an elongated morphology that stretched from apical to basal surface over the course of imaging and later differentiative divisions (D-divisions) occurred at the apical (ventricular) surface (Figure 4A). However, in *nok* morphant tissue, cells were not separated across the midline and they appeared clumped together, often in rosette-like

structures. D-divisions in *nok* morphants occurred within these cell clumps, at a distance from the midline of the tissue (Figure 4B and quantified in 4C). This was in contrast to their WT counterparts which divided strictly adjacent to the lumen (apical) surface. The cell behaviour of ectopic divisions in *nok* morphants is accompanied by a lateral dispersal of Pard3 expression from the midline (Figure 4D). Thus, as well as being unable to undergo the puncta-to-apical ring transition (Figure 1E), Nok deficient cells show persistent adhesions and the tissue organisation becomes progressively fragmented over time.

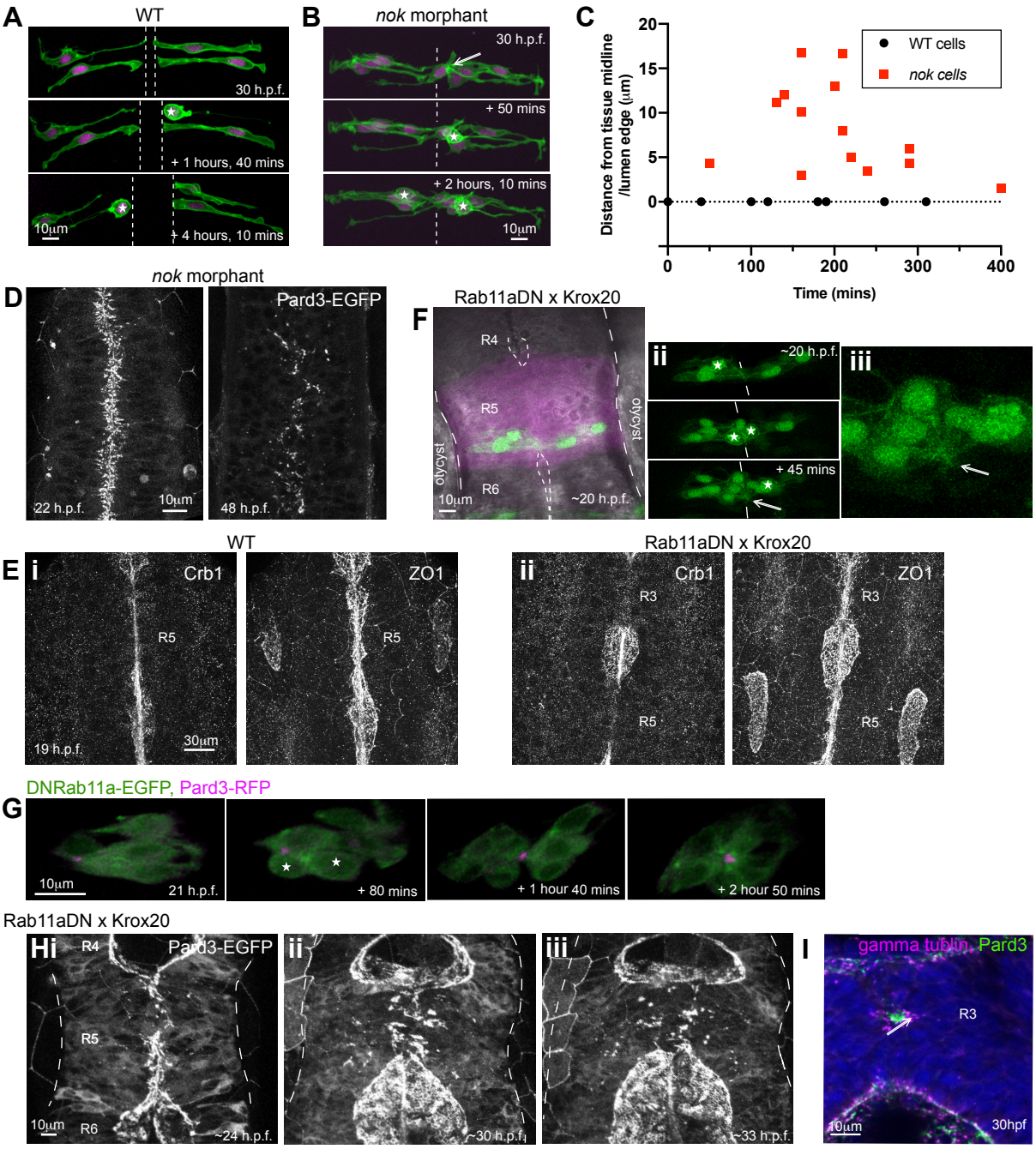


**Figure 4. Persistent adhesion in Nok and Rab11a deficient cells**
**A)** Images from a time-lapse movie of mosaically labelled neuroepithelial cells in the hindbrain of a 25 h.p.f. WT embryo in dorsal orientation. Cells have separated across the tissue midline and the lumen

has opened (short dotted lines). D-divisions (stars) occur at the apical surface (8/8 cells) and cells re-established an elongated morphology towards the basal surface following division (14/14 cells).
**B)** Images from a time-lapse movie of mosaically labelled neuroepithelial cells in the hindbrain of a 25 h.p.f. *nok* morphant embryo in dorsal orientation. Cells have failed to separate across the tissue midline (dotted line) and formed clumps (sometimes with a rosette-like structure, arrow. D-divisions (stars) occurred near the centre of the cell clumps, which was often not situated near the tissue midline (9/14 cells from 2 groups divided basal to the midline). 50% cells failed to re-establish an elongated morphology towards the basal surface following division (13/26 cells).
**C)** Graphical representation of division locations of individual cells in relation to the tissue midline or lumen edge over time from 30 h.p.f. All wild type cells that had separated across the midline divided exactly at the lumen edge. All *nok* morphant cells that had not separated divided distal to the tissue midline.
**D)** 10µm Z-projection in dorsal orientation at a mid dorso-ventral level through the hindbrain of *nok* morphant Pard3-EGFP embryos at 22 h.p.f. and 48 h.p.f. At 22 h.p.f. Pard3-EGFP was localised near the tissue midline but did not form continuous straight expression domains as seen in wild types (Figure 3Ai) and the lumen failed to open. By 48 h.p.f. Pard3-EGFP localisation became fragmented into clumps.
**E)** 70-80µm Z-projections in dorsal orientation in the hindbrain of 19 h.p.f. embryos. **i.** Wild-type embryo. Both Crumbs 1 (Crb1) and Zonula Occludens 1 (ZO1) were localised to the apical midline (n=3/3). **ii.** Embryo in which UAS:DNRab11a was expressed under the Krox20:KalTA4 activator in rhombomeres 3 and 5 (DNRab11a x Krox20). ZO1 was localised to the midline but Crb1 was largely absent from rhombomeres 3 and 5 (n=3/3).
**F) i.** 11 µm Z-projection in dorsal orientation of mosaically labelled neuroepithelial cells in the hindbrain of a 20 h.p.f. Single z-section in greyscale and 52µm projection in magenta denoting rhombomere 5 for reference. Long dotted lines denote basal surfaces. The lumen in rhombomere 5 has failed to open but has started to open in rhombomeres 4 and 6 (short dotted lines).
**ii.** Images from a time-lapse movie of cells in i which have failed to separate across the tissue midline. Following D-divisions (stars), cells remain attached and arrange into a rosette-like structure (arrow), enlarged in **iii**.
**G)** 3D reconstruction of a time-lapse of mosaically distributed DNRab11a-EGFP neuroepithelial cells in the hindbrain of a 24 somite-stage (equivalent to 21 h.p.f.) embryo. Following division cells do not separate and form a rosette around a centrally located puncta of Pard3-RFP.
**H)** Approximately 70 µm Z-projections from a time-lapse movie through a DNRab11a x Krox20 embryo hindbrain labelled with Pard3-EGFP fusion protein, starting at approximately 24 h.p.f. In the same way as in *nok* morphants in figure 4D and as previously reported (Buckley et al. 2013), Pard3 was initially localised near the tissue midline of rhombomere 5 but the lumen failed to open and Pard3 localisation became fragmented into clumps that were localised progressively further from the tissue midline.
**I)** 4 µm Z-projection in dorsal orientation 23 µm below the rhombomere surface of a 30 h.p.f. DNRab11a x Krox20 embryo hindbrain at rhombomere 3, stained via IHC for Pard3 and gamma-tubulin. Pard3 is localised in a round clump, surrounded on all sides by centrosomes.

Since we hypothesise that Nok functions through its ability to localise Crumbs to the nascent apical surface, we next analysed cell behaviours following another manipulation that depletes Crumbs from the apical surface. For this we expressed a dominant-negative (DN) form of Rab11a in rhombomeres 3 and 5. We previously showed that this manipulation reduces apical Crumbs 2a localisation and prevents lumen opening in these segments (Buckley et al., 2013). Here, we show that apical Crumbs 1 is also downregulated in DNRab11a rhombomeres (Figure 4E), confirming that this manipulation is sufficient to downregulate apical trafficking of multiple Crumbs paralogs. We found that cells in the DNRab11a rhombomeres did not separate following D-division, progressively forming cell clumps and rosette-like structures (Figure 4F). An example of rosette formation around a central focus of Pard3 is depicted in Figure 4G. Similar to *nok* morphants (Figure 4D), at a tissue level, a lateral dispersal of Pard3-

EGFP from the midline was seen, progressively fragmenting the midline organisation over time (Figure 4H). This was similar to our previous observations of ZO-1 dispersion in DNRab11a segments (Buckley et al., 2013). IHC staining of DNRab11a rhombomeres revealed rosette-like structures with centrally located ectopic apical proteins surrounded by centrosomes (Figure 4I).

Interestingly, whilst cells situated in the middle of closed-lumen DNRab11a rhombomeres 3 and 5 formed clumps, cells at the edges of these rhombomeres had a typical elongated neuroepithelial morphology and were able to build an aPKC positive apical surface that was contiguous with the wild-type apical surface in adjacent open-lumen wild-type rhombomeres 2, 4 and 6 (Figure 5A). Edge cells were oriented obliquely along the anterior-posterior axis of the embryo, apical towards the open lumens (e.g. arrows in figure 5Aii). To determine how this morphology arose, we made time-lapse movies of DNRab11a/wild-type interface neuroepithelial cells. We found that interface cells remained connected across the midline as the neighbouring wild-type lumen inflated, acting like a hinge and reorienting the cells at the boundary between DNRab11a and wild-type rhombomeres towards the opening lumen (Figure 5Bi). Despite these persistent connections between cells, the DNRab11a luminal surface expanded via cell division and subsequent reintegration into the epithelium (Figure 5Bii.)

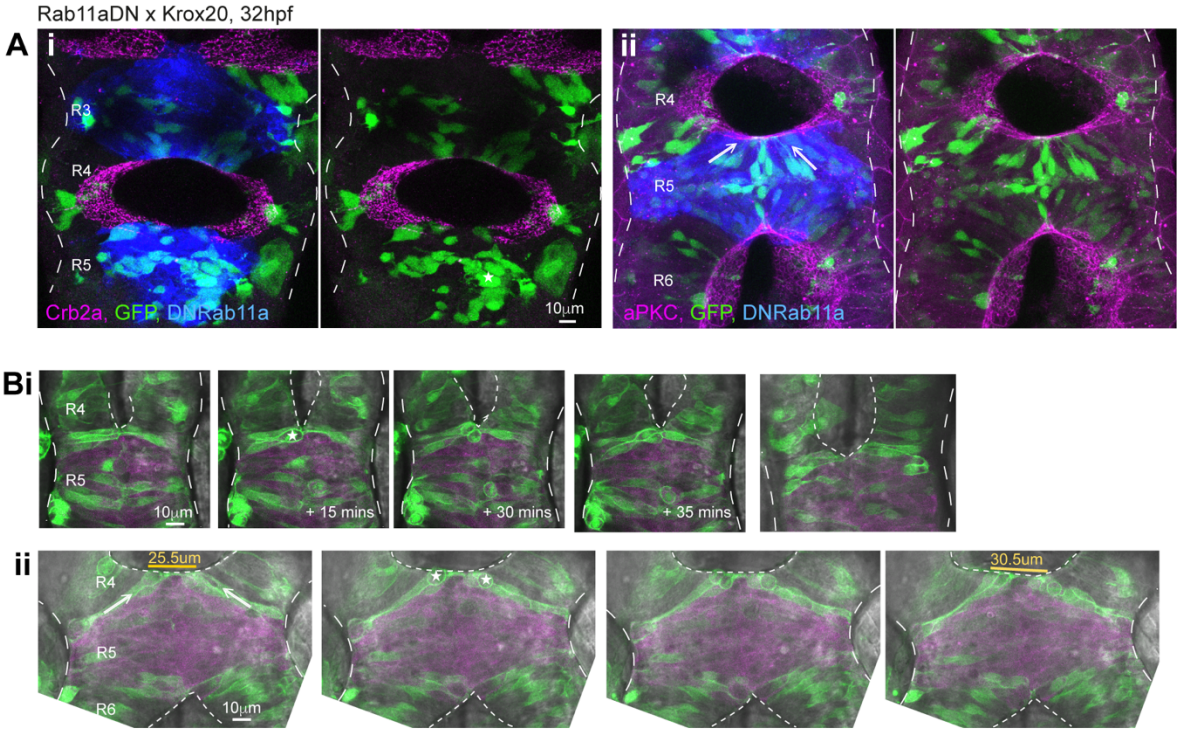


**Figure 5. Cells at the WT/DNRab11a interface contribute to the luminal surface**

**A)** 15-18μm z-projections through 32 h.p.f. DNRab11a x krox20 embryo hindbrains stained by IHC for Crb2a (i) or aPKC (ii). Cells are mosaically labelled with cytoplasmic GFP and H2A-GFP.

**i.** Crb2a is largely (but not completely) absent from DNRab11a apical regions (5/5 embryos).
**ii.** aPKC is present around the whole apical surface of both wild-type and DNRab11a rhombomeres (4/4 embryos). Cells situated in the centre of DNRab11a rhombomeres clumped together (e.g. star in i) whilst cells in contact with the open lumens had elongated morphology (e.g. arrows in ii).
**B)** Single Z-slices from a timelapse movies in dorsal orientation of mosaically labelled neuroepithelial cells in rhombomere 5 of approximately 24 h.p.f. DNRab11a x Krox20 embryos over time. Long dotted lines denote basal surfaces. Short dotted lines denote apical surfaces.
**i)** As the neighbouring lumen inflated, cells at the edge of the DNRab11a rhombomere remained connected across the midline and cells divided at this central point of connection (star).
**ii)** As the neighbouring lumen inflated further, cells near the WT/DNRab11a interface reoriented towards the open lumen (e.g. arrows). Cells divided at the WT/DNRab11a interface (stars) and reintegrated into the epithelium, widening the DNRab11a surface in contact with the neighbouring lumen (see measurements in orange).

These results demonstrate that DNRab11a cells at the DNRab11a/wild-type interface are able to remain integrated into an epithelium if they have access to an apical lumen surface. Together, our data suggests that persistent adhesion between cells not only inhibits lumen opening but may also contribute to the lack of epithelial maintenance in both Nok deficient and DNRab11a embryos, resulting in a gradual fragmentation of midline organisation.

**Nok is necessary for apical ring formation even in the absence of cell division.**

A recent paper's analysis of cell divisions and lumen formation in *nok*$^{m520}$ mutants suggested that Nok/Crumbs function in lumen formation may be specifically related to resolving connections between sister cells following the C-division (Guo et al., 2018). In the course of analysing junction formation in *nok*$^{m227}$ mutants, we uncovered that the loss of lumen formation itself in these mutants was more complicated than expected. In line with previous observations (Lowery et al., 2009, Lowery & Sive, 2005), we found the loss of lumen formation was not fully penetrant and consistently found small lumens formed at the level of the midbrain hindbrain boundary (Figure 6A), and less frequently small lumens in the dorsal aspects of the hindbrain at the level of the otic vesicles. We found that Crumbs protein was present at the apical surface of these small lumens (Figure 6B), providing further evidence for the role of Crumbs in the successful formation of an apical surface and opening of a lumen

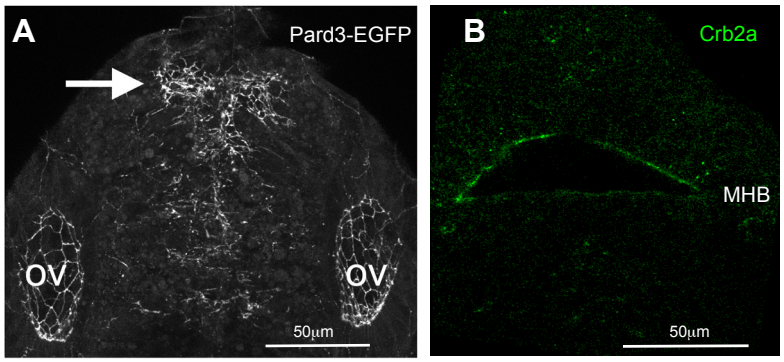


**Figure 6. *nok*$^{m227}$ mutants still open a lumen at the MHB**
A. A 57µm maximum projection of Z-stack of the hindbrain neural rod from a 28 somite stage *nok*$^{m227}$ mutant; Pard3-EGFP compound transgenic embryo at the level of the otycysts. Apical rings have formed at the mid-hindbrain boundary (MHB, arrow).

B. Single horizontal Z-plane of the hindbrain neural rod from a *nok*$^{m227}$ mutant embryo at the level of the MHB, imaged for Crb2a immunoreactivity. A lumen has opened, which is lined with Crumbs2a protein apically.

Since the closed-lumen phenotype is not fully penetrant in *nok* mutants, we suggest that analysing the rescue of the open lumen phenotype is problematic in *nok*. To better analyse whether Nok has specific functions in relation to the C-division we therefore analysed apical ring formation in the anterior spinal cord. This region is distant from the midbrain hindbrain boundary and the level of otic vesicles and provides a more reliable and precise assay of Nok function.

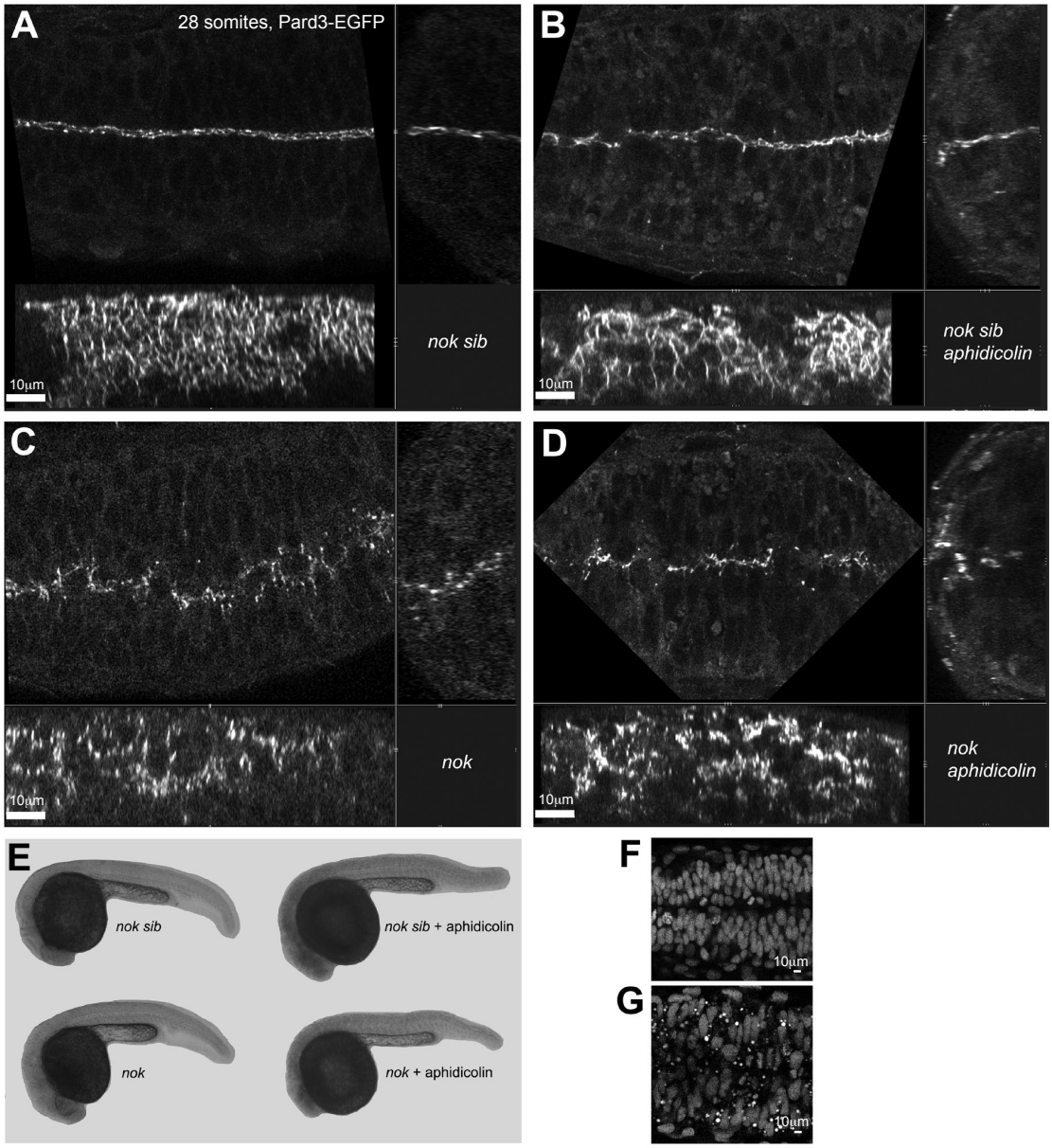


**Figure 7. Nok is necessary for apical ring formation even in absence of cell division.**

**A)** Orthogonal series of horizontal (top left), transverse (top right) and sagittal (bottom) confocal planes of Pard-EGFP expression in a wildtype sibling from a *nok* mutant clutch of embryos.

**B)** Orthogonal series of horizontal, transverse and sagittal confocal planes of Pard-EGFP expression in a wildtype sibling from a *nok* mutant clutch of embryos that has been treated with aphidicolin to block the C-divisions.
**C)** Orthogonal series of horizontal, transverse and sagittal confocal planes of Pard-EGFP expression in a *nok* mutant embryo.
**D)** Orthogonal series of horizontal, transverse and sagittal confocal planes of Pard-EGFP expression in a *nok* mutant embryo treated with aphidicolin to block C-divisions.
**E)** Overall body shape of wildtype siblings and *nok* mutants with and without aphidicolin treatment.
**F)** Horizontal section through neural tube showing nuclear staining in wildtype embryo.
**G)** Horizontal section through neural tube showing nuclear staining in wildtype embryo treated with aphidicolin, so show larger nuclei due to division block.
All embryos are at 28 somite stage

We have shown that Nok and Rab11a are required for cells to separate across the midline following the C-division. We have previously demonstrated that left-right separation was not rescued by blocking division in DNRab11a embryos, suggesting that the role of Rab11a/Crumbs is not exclusively related to cell-cell separation between sister cells (Buckley et al., 2013). To address whether Nok/Crumbs function may be specifically related to resolving connections between sister cells (as suggested in Guo et al. 2018), we analysed the key events of apical ring formation in *nok*$^{m227}$ mutant embryos with and without C-divisions. We blocked C-divisions using the S-phase inhibitor Aphidicolin as described previously (Guo et al., 2018, Lyons et al., 2005) and analysed Pard3-GFP expression in the anterior spinal cord region. Apical rings of Pard3-EGFP are not rescued by blocking C-divisions in *nok*$^{m227}$ mutants (n = 6/6 embryos, Figure 7A - D). The efficacy of the division block was confirmed by the enlarged nuclear size in aphidicolin treated embryos (Figure 7F and G) and the enlarged size of the apical rings in the aphidicolin treated nok siblings (Figure 7B). These results demonstrate that Nok function is not specifically related to remodelling adhesions between C-division sisters. Our results show that Nok plays a more fundamental role in the formation of apical junctional rings and release of contralateral adhesions during *de novo* polarisation of an epithelial tube.

## Discussion

Our work uncovers three aspects of *de novo* apical surface generation within a complex organ *in vivo*. First despite the very different cellular organisations, apical surface generation at the centre of a solid organ primordium follows a strikingly similar sequence of spot to ring junction building to those previously described for apical surface generation at a free surface of a sheet of cells. Second the displacement of proteins from the nascent apical surface to the nascent apicolateral junctional belt domain serves two purposes in a solid organ primordium; it simultaneously contributes to the building of epithelial junctional belts and releases adhesions with contralateral cells that would otherwise inhibit the generation of a free surface and lumen

formation. Our comparable results in *nok* mutant/morphant and DNRab11a tissue lead us to propose that the correct apical localisation of Crumbs protein is necessary for both apical ring formation and the resolution of adhesions between cells. Thirdly cell divisions across the nascent apical plane drive local cell-cell rearrangements that draw ipsilateral and contralateral junctions to the straightening left-right interface and contribute to the offset alignment of contralateral cells across the midline. At single cell resolution pairs of sister cells do not remain connected '*en face*' as previously suggested (Guo et al., 2018), but instead sisters become attached in an offset configuration from one another across the midline. In addition, we address a recent suggestion that the MAGUK scaffolding protein Nok is only required to remodel apical protein location following cell divisions across the nascent apical plane (Guo et al., 2018). We show this is not the case as Nok-dependent apical protein remodelling is required for apical surface generation both with and without cell divisions.

**The roles of Nok, Rab11a and Crumbs**

The transmembrane protein Crumbs is an essential determinant of apical organisation. In Drosophila ectoderm, Crumbs is required during epithelial sheet development to displace Bazooka (Drosophila Pard3), from the nascent apical surface to the apicolateral cell border (Morais-de-Sa et al., 2010). In turn, Bazooka is required to reposition the transmembrane adhesion protein Drosophila E-cadherin (DE-cadherin), thus building the apicolateral junctional belts that tie the epithelial cells together (McGill et al., 2009, Pilot et al., 2006, St Johnston & Ahringer, 2010, Wei et al., 2005). Here, we describe a similar displacement of Pard3 and repositioning of the main zebrafish neuroepithelial cadherin, Cdh2, to the apicolateral cell borders in the zebrafish neural rod and show that Nok/Mpp5 is necessary for this displacement and for the formation of apical rings. We propose Nok operates here through its role in scaffolding Crumbs proteins at the apical surface, as Crumbs has been shown to be necessary for spot to ring formation in *Drosophila* ectoderm (e.g. Roeth et al., 2009, Tepass, 1996). A direct test of Crumbs function is difficult in zebrafish because three different Crumbs proteins (Crb1, Crb2a and Crb2b) are present at this stage in the developing neural rod. Previous research has shown that neuroepithelial organisation is only altered when all paralogs of Crumbs protein were knocked down by multiple morpholinos (Zou *et al.* 2013) and, consistent with our hypothesis, this appears to include a lack of lumen formation. Rather than transiently knocking down all paralogs of Crumbs proteins in this study, we used stable genetic manipulations of Nok and Rab11a that downregulate all paralogs of Crumbs protein from the nascent apical surface. Both Nok and Rab11a manipulations show persistent contralateral adhesions, lack of lumen opening and comparable disorganisation of neuroepithelial tissue at later stages (Figure 4).

In the case of the zebrafish neural rod, this primordium is initially a solid tissue, so the displacement of Pard3 and Cdh2 is not from a free apical surface but instead occurs within the densely packed cell-cell interfaces that lie at the centre of the rod. Cell adhesions between contralateral cells across the neural rod centre initially bind the left and right halves of the neural rod together, but these adhesions need to be released to generate the lumen and apical surface of the neural tube. In support of the role of Crumbs protein in building apical junctions within the solid neural rod we characterised cell behaviour and epithelial maintenance in both *nok*$^{m227}$ mutants and morphants (which are unable to assemble all forms of Crumbs at the apical surface, Zou *et al.* 2013) and in cells with non-functional Rab11a (which are unable to transport Crumbs protein to the apical surface, e.g. Roeth *et al.* 2009, Buckley *et al.,* 2013). In both cases we found that cells were unable to release cell-cell adhesions. During epithelialisation of the neural rod, this first resulted in closed lumens. At later stages, when neuroepithelial cells undergo interkinetic nuclear migration during D-divisions, this resulted in progressive disintegration of epithelial organisation. We propose this is likely due to a combination of factors - cells were unable to separate following divisions, interkinetic nuclear migration and mitotic rounding pulls cells around within the tissue and the lack of apical junctional rings fails to hold cells at what should be the apical surface.

These results show Nok and Rab11a, likely operating through the localisation of the transmembrane protein Crumbs to the nascent apical surface, neatly coordinates the release of contralateral connections with the strengthening of ipsilateral connections, thus leading both to the generation of a free surface within the centre of an initially solid tissue and to epithelialisation. Our results suggest that resolution of cell adhesions is necessary both for midline lumen opening and for maintaining an organised epithelium later in development. This leads us to postulate that a lack of cell-cell separation may contribute to other reported epithelial disorganisation phenotypes in Crumbs or Rab11a-deficient epithelia (e.g. Das & Knust, 2018, Roeth et al., 2009).

By studying dominant-negative Rab11a cells in an environment where they have access to wildtype neighbours, we also uncovered that cells depleted of Crumbs from their apical surface can none-the-less form an epithelial surface when adjacent to wildtype cells. Thus, in the fish neuroepithelium, Rab11a and Crumbs appear to be required for *de novo* epithelial surface generation but dispensable for integration next to an already generated apical surface. This suggests that non cell-autonomous rescue from neighbouring wildtype cells is able to initiate epithelialisation in the absence of Rab11a/Crumbs.

**The role of the C-division**

A recent paper also concluded that Nok is necessary to remodel junctional proteins during epithelialisation in the neural rod (Guo et al., 2018). They however propose that Nok's role in apical remodelling is only necessary to rescue the tissue disruption caused by midline C-divisions, a conclusion based on their reported rescue of lumen formation and apical junctional belts when cell division is blocked in the *nok*$^{m520}$ mutant. However, we show that blocking cell division does not rescue junctional belt formation in *nok*$^{m227}$ mutants (Figure 7), and thus has a more fundamental role in apical junction remodelling than resolving the potential disruption to tissue organisation caused by C-divisions. We suggest the results of Guo et al (2018) may be a consequence of their use of the weaker *nok*$^{m520}$ mutant allele having non-penetrant phenotypes, as they previously published (Zou et al., 2013). We further suggest the mini-lumen at the midbrain-hindbrain boundary that we observed in *nok*$^{m227}$ mutants (Figure 6) is due to the expression of a second Nok-like gene expressed in this region (such as Mpp2b, Thisse & Thisse, 2004). Nok/Mpp5a is a member of the Mpp MAGUK protein family and there are 6 Mpp genes (MPP2-MPP7) with conserved protein domain structure. All of these genes contain a PDZ domain, which in the case of Nok (or Pals1), has been shown to be the specific domain that binds Crumbs (Roh et al., 2002). Little is known about the other mpp genes in zebrafish and this could form the basis of further study.

We have previously demonstrated that C-divisions at the midline of the neural rod are an important morphogenetic force during neural tube formation. Ectopic divisions are able to organise ectopic neural lumens and duplicate the neural tube (Tawk et al., 2007) while neural tubes generated in the absence of midline C-divisions are less efficient at resolving cell interdigitation across the midline and have a disorganised morphology (Buckley et al., 2013). Here we show that Cdh2 junctions between ipsilateral and contralateral cells are pulled into the cleavage furrow of midline C-divisions thus integrating left-right connections into a restricted sagittal plane (Figure 2). This ingression of neighbours into the cleavage furrow is strikingly reminiscent of neighbour ingression during mitoses in *Drosophila* epithelia (Wang et al., 2018) and of cytokinesis-mediated cell intercalation reported during chick gastrulation (Firmino et al., 2016). The consequent alignment of cell adhesions between neighburing cells is likely to be one way that C-divisions confer a morphogenetic advantage in midline formation. The maintenance of connections with multiple contralateral cells through C-divisions ensures that cells do not solely connect to their sisters and connections across the midline thus become staggered. We propose that this staggered alignment of endfeet may generate a morphogenetic advantage since it allows the attachment to a larger number of cells than a one-to-one 'mirror adhesion' as has previously been proposed (Guo et al., 2018), and therefore helps colocalise apical junctions from multiple neighbouring cells to the tissue

midline. The localisation of junctional proteins at cell corners might also be important for allowing flexibility of cell movement during tissue remodelling (e.g. Finegan et al., 2019).

## Methods

### Embryo Care

All embryos were collected, staged and cultured according to standard protocols (Kimmel et al., 1995). All procedures were carried out with UK Home Office approval and were subject to local Ethical Committee review.

### Generation of Pard3-EGFP transgenic line

To generate the transgenic zebrafish line expressing Pard3-EGFP with endogenous spatial and temporal expression we used bacterial artificial chromosome (BAC) recombineering. We replaced the stop codon of the pard3-003/ASIP transcript (von Trotha et al., 2006), in the BAC clone DKEY-71E21 (Source Bioscience). This BAC clone contains ~71 kb upstream of the pard3-003/ASIP start codon and ~30 kb downstream from the targeted stop codon. We followed the protocol of (Bussmann & Schulte-Merker, 2011), with some modifications. The original protocol leaves a kanamycin selection cassette in the final BAC construct. However, we found this led to cell death and a lack of endogenous Pard3-EGFP expression. To remove the kanamycin selection cassette, we substituted two reagents with those from the Sarov *et al.,* 2006 recombineering protocol and added an extra 'flip out' step to remove the kanamycin cassette. Specifically, we used the pRedFlp4 and R6k-EGFP-FRT-kanR-FRT cassettes from Sarov *et al* 2006. The EGFP-FRT-kan-FRT targeting cassette was PCR amplified with 50 bp homology arms at either end, to target it to replace the pard3-003/ASIP stop codon during BAC recombineering.

Forward primer:

5'-CACAGAAGCAGAACGGACGCAATGGACACCCCTCCACTTCAGACAGGTAC**AGCTCAGGAGGTAGCGG** -3'

and reverse primer:

5' -AATTGAGTTTCATGATAGAACTTTGTATTTCTGCAATTCTGAAAAGCTGA**GGCAGATCGTCAGTCAG** -3'.

The protocol for pRedFlp4 transformation, targeted recombination steps and removal of the kanamycin resistance selection marker by pRedFlp4 induced flipase were carried out as previously described (Sarov et al., 2006), with slight modifications. Briefly, the recombineering pipeline was modified to have two rounds of tagging by Red/ET recombination, the first was insertion of iTol2_amp into the BAC backbone and the second insertion of EGFP-FRT-kanR-FRT. Successful recombination was assessed by colony PCR and then full sequencing of the sites of recombination. Preparation and injection of BAC DNA and screening for transgenic founders was all performed according to standard protocols (Bussmann & Schulte-Merker, 2011, Suster et al., 2011).

**Zebrafish Lines**

The TgBAC(pard3:Pard3-EGFP)$^{kg301}$ was generated as detailed above. The TgBAC(cdh2:Cdh2-tFT) (Revenu et al., 2014), was kindly provided by Darren Gilmour. The TgBAC(cdh2:Cdh2-tFT) line expresses both Cdh2-sfGFP and Cdh2-tagRFP, but we only image Cdh2-sfGFP expression in our experiments and refer to this as Cdh2-GFP for simplicity. These lines were bred with the Nok$^{m227}$ mutant fish line (Wei & Malicki, 2002a) to generate compound Nok$^{m227}$; Cdh2-tFT and Nok$^{m227}$; Pard3-EGFP fish. To prevent ventricle opening in rhombomeres 3 and 5, we crossed the UAS-inducible dominant-negative Rab11a line, Tg(UAS:mCherry-Rab11a S25N)$^{mw35}$ (Clark et al., 2011), with Tg(Krox20:RFP-KalTA4), which drives the optimised Gal4-activator, KalTA4, only in Krox20 positive rhombomeres 3 and 5 (Distel et al., 2009). This resulted in the expression of Rab11a-S25N specifically in rhombomeres 3 and 5 as previously described (Buckley et al., 2013).

**RNA preparation and injection**

Fusion constructs containing cDNA in the pCS2+ vector were linearized and mRNA was synthesised using the SP6 mMessage mMachine kit (Ambion, AM1340). RNA for the following constructs was injected using standard protocols (Westerfield, 2000) at 40-100pg per embryo: Histone 2A tagged with GFP (H2A-GFP), Human Histone 2B tagged with RFP (H2B-RFP), Human CAAX membrane moiety tagged with EGFP, mCherry or mNeptune2.5 (EGFP-CAAX, mCherry-CAAX, mNeptune2.5-CAAX), Dominant-negative Human rab protein 11a tagged with EGFP (RAB11A-S25N-EGFP), Zebrafish partitioning-defective 3 tagged with GFP or RFP (Pard3-GFP/RFP). For ubiquitous distribution of mRNA, embryos were injected at 1-2 stage. For mosaic labelling a single blastomere of a 16-64 cell stage embryo was injected.

**Morpholino injections**

Co-injection of 0.5 nL of *nok* splice blocking morpholinos (final concentration of 300 μM each; donor: 5'- GTT TAT GAC ACC CAC CTA GTA AAG C -3' and acceptor: 5'- CTC CAG CTC TGA AAG TAC AAA CAC A -3'), was injected into one-cell stage embryos (Hsu et al., 2006). Nok morpholinos recapitulate the Nok mutant phenotype (this manuscript and Hsu *et al.* 2006).

Cell division during neurulation was blocked by injecting embryos with 0.5 nL of 0.5 mM *emi1* ATG splice blocking morpholino at the one-cell stage (Buckley et al., 2013). Blocking *emi1* was previously shown to arrest cells in the G2 phase of the cell cycle (Rhodes et al., 2009, Zhang et al., 2008). Control embryos were injected with standard control morpholino at the same concentration and stage.

**Chemical inhibition of cell division**

Cell division was blocked by incubating dechorionated embryos in a combination of 150 μM aphidicolin (Sigma) and 20 mM hydroxyurea (Sigma) in 4% DMSO from bud stage (10 hpf) to 26 ss (22 hpf) (Guo et al., 2018, Lyons et al., 2005). Embryos were maintained on a bed of agarose in 12-well plates in the dark throughout the drug incubation. The drug combination used was previously shown to take 4 hours for it to be most effective, from which point it almost completely blocks cell division (Lyons et al., 2005).

**Immunohistochemistry**

Embryos were fixed with 4% paraformaldehyde for 2 hours at room temperature prior to processing for immunohistochemistry. The following primary antibodies were used: mouse anti-Crb2a (mouse monoclonal, ZIRC zs-4, 1:200 ), rabbit anti-Crb2a and anti-Crb1 (a kind gift from the Wei lab, 1:350), mouse anti-ZO-1 (mouse monoclonal, Invitrogen 33-9100, 1:500), rabbit anti-aPKC (rabbit polyclonal, Santa Cruz sc-216, 1:300), mouse anti-γtubulin (mouse monoclonal, MilliporeSigma T6557, 1:200) and mouse anti-ZO-1 (Life Technologies, 1:300). Rabbit anti-Pard3 (rabbit polyclonal, Millipore 07-330, 1:100) was used following fixation in Dent's for 3 hours at room temperature and rehydration from methanol. AlexFluor secondary antibodies (Life Technologies) were used at 1:500 and Hoeshct (Life Technologies) nuclei stain was used at a final concentration of 1:10,000.

**Confocal imaging and processing**

Embryos were mounted in low melting point agarose and imaged using a Zeiss LSM 880 Fast Airyscan microscope and water dipping x20/1.0 N.A. objective and a Leica SP5 confocal microscope and water dipping x25/0.95 N.A objective. Imaging at the centre of a developing live tissue mass required the improved resolution in x, y and z obtained by using the Fast

Airyscan mode of the Zeiss LSM 880 Fast Airyscan microscope. By using this microscope, high-resolution images of both *en face* Pard3-EGFP rings and the spatial location of Crb2a, aPKC and Cdh2-EGFP in the developing embryo were obtained. To further improve lateral imaging, fish were mounted on an agarose bed with small depressions to hold the yolk of the embryo in place. These agarose beds were made using a custom mould (a kind gift from Andrew Oates). Data was collected from the hindbrain and anterior spinal cord regions. Some adjacent cells have been removed from images of single cells to increase clarity of the cells of interest. Images were processed using Imaris, Volocity and Fiji/ImageJ.

**Electron microscopy**

Embryos were fixed in 2% paraformaldehyde and 1.5% glutaraldehyde in 0.1M sodium cacodylate buffer over-night and then processed through 1% osmium and stained in 0.5% uranyl acetate. They were then dehydrated in ethanol and processed through propylene oxide into 100% resin, embedded and baked. Ultra-thin sections were taken in transverse orientation and imaged on a transmission electron microscope.

**Acknowledgements**

We thank Rachel Moore, Christopher Rookyard, Vineetha Vijayakumar and Xuan Liang for helpful discussions on this work. We thank Darren Gilmour for the Cdh2:(Cdh2-tFT) line, Gwyn Gould for RAB11A-S25N-EGFP plasmid and Xiangyun Wei for the Crb2a antibody. This work was supported by UK BBSRC grant BB/K000926/1 (JC), a Wellcome Trust Investigator Award (JC) and a Wellcome Trust/ Royal Society Sir Henry Dale Fellowship (CB).

**Author contributions**

Conceptualization: AS, CB, JC

Investigation: AS, CB, CW, JC

Writing, reviewing & editing: AS, CB, JC

Supervision: CB, JC

Funding acquisition: CB, JC

## References


Buckley CE, Ren X, Ward LC, Girdler GC, Araya C, Green MJ, Clark BS, Link BA, Clarke JDW (2013) Mirror-symmetric microtubule assembly and cell interactions drive lumen formation in the zebrafish neural rod. EMBO J 32: 30-44

Bussmann J, Schulte-Merker S (2011) Rapid BAC selection for tol2-mediated transgenesis in zebrafish. Development 138: 4327-32

Clark BS, Winter M, Cohen AR, Link BA (2011) Generation of Rab-based transgenic lines for in vivo studies of endosome biology in zebrafish. Dev Dyn 240: 2452-2465

Das S, Knust E (2018) A dual role of the extracellular domain of. Biol Open 7

Distel M, Wullimann MF, Koster RW (2009) Optimized Gal4 genetics for permanent gene expression mapping in zebrafish. Proc Natl Acad Sci U S A 106: 13365-13370

Finegan TM, Hervieux N, Nestor-Bergmann A, Fletcher AG, Blanchard GB, Sanson B (2019) The tricellular vertex-specific adhesion molecule Sidekick facilitates polarised cell intercalation during Drosophila axis extension. PLoS Biol 17: e3000522

Firmino J, Rocancourt D, Saadaoui M, Moreau C, Gros J (2016) Cell Division Drives Epithelial Cell Rearrangements During Gastrulation in Chick. Dev Cell 36(3): 249-261

Grawe F, Wodarz A, Lee B, Knust E, Skaer H (1996) The Drosophila genes crumbs and stardust are involved in the biogenesis of adherens junctions. Development 122: 951-9

Guo C, Zou J, Wen Y, Fang W, Stolz DB, Sun M, Wei X (2018) Apical Cell-Cell Adhesions Reconcile Symmetry and Asymmetry in Zebrafish Neurulation. iScience 3: 63-85

Harris TJ, Peifer M (2005) The positioning and segregation of apical cues during epithelial polarity establishment in Drosophila. J Cell Biol 170: 813-23

Hsu Y-C, Willoughby JJ, Christensen AK, Jensen AM (2006) Mosaic Eyes is a novel component of the Crumbs complex and negatively regulates photoreceptor apical size. Development 133: 4849-4859

Kimmel CB, Ballard WW, Kimmel SR, Ullmann B, Schilling TF (1995) Stages of embryonic development of the zebrafish. Dev Dyn 203: 253-310

Kimmel CB, Warga RM, Kane DA (1994) Cell cycles and clonal strings during formation of the zebrafish central nervous system. Development 120: 265-276

Lowery LA, De Rienzo G, Gutzman JH, Sive H (2009) Characterization and classification of zebrafish brain morphology mutants. Anatomical record (Hoboken, NJ : 2007) 292: 94-106

Lowery LA, Sive H (2005) Initial formation of zebrafish brain ventricles occurs independently of circulation and requires the nagie oko and snakehead/atp1a1a.1 gene products. Development 132: 2057-2067

Lyons DA, Pogoda H-M, Voas MG, Woods IG, Diamond B, Nix R, Arana N, Jacobs J, Talbot WS (2005) erbb3 and erbb2 are essential for schwann cell migration and myelination in zebrafish. Curr Biol 15: 513-524

McGill MA, McKinley RF, Harris TJ (2009) Independent cadherin-catenin and Bazooka clusters interact to assemble adherens junctions. J Cell Biol 185: 787-96

Morais-de-Sa E, Mirouse V, St Johnston D (2010) aPKC phosphorylation of Bazooka defines the apical/lateral border in Drosophila epithelial cells. Cell 141: 509-23

Pilot F, Philippe JM, Lemmers C, Lecuit T (2006) Spatial control of actin organization at adherens junctions by a synaptotagmin-like protein Btsz. Nature 442: 580-4

Revenu C, Streichan S, Donà E, Lecaudey V, Hufnagel L, Gilmour D (2014) Quantitative cell polarity imaging defines leader-to-follower transitions during collective migration and the key role of microtubule-dependent adherens junction formation. Development 141: 1282-1291

Rhodes J, Amsterdam A, Sanda T, Moreau LA, McKenna K, Heinrichs S, Ganem NJ, Ho KW, Neuberg DS, Johnston A, Ahn Y, Kutok JL, Hromas R, Wray J, Lee C, Murphy C, Radtke I, Downing JR, Fleming MD, MacConaill LE et al. (2009) Emi1 maintains genomic integrity during zebrafish embryogenesis and cooperates with p53 in tumor suppression. Mol Cell Biol 29: 5911-5922

Roeth JF, Sawyer JK, Wilner DA, Peifer M (2009) Rab11 helps maintain apical crumbs and adherens junctions in the Drosophila embryonic ectoderm. PLoS One 4: e7634

Roh MH, Makarova O, Liu CJ, Shin K, Lee S, Laurinec S, Goyal M, Wiggins R, Margolis B (2002) The Maguk protein, Pals1, functions as an adapter, linking mammalian homologues of Crumbs and Discs Lost. J Cell Biol 157: 161-72

Sarov M, Schneider S, Pozniakovski A, Roguev A, Ernst S, Zhang Y, Hyman AA, Stewart AF (2006) A recombineering pipeline for functional genomics applied to Caenorhabditis elegans. Nat Methods 3: 839-44

St Johnston D, Ahringer J (2010) Cell Polarity in Eggs and Epithelia: Parallels and Diversity. Cell 141: 757-774

Suster ML, Abe G, Schouw A, Kawakami K (2011) Transposon-mediated BAC transgenesis in zebrafish. Nat Protoc 6: 1998-2021

Tawk M, Araya C, Lyons DA, Reugels AM, Girdler GC, Bayley PR, Hyde DR, Tada M, Clarke JD (2007) A mirror-symmetric cell division that orchestrates neuroepithelial morphogenesis. Nature 446: 797-800

Tepass U (1996) Crumbs, a component of the apical membrane, is required for zonula adherens formation in primary epithelia of Drosophila. Dev Biol 177: 217-25

Thisse B, Thisse C (2004) Fast Release Clones: A High Throughput Expression Analysis. ZFIN Direct Data Submission

von Trotha JW, Campos-Ortega JA, Reugels AM (2006) Apical localization of ASIP/PAR-3:EGFP in zebrafish neuroepithelial cells involves the oligomerization domain CR1, the PDZ domains, and the C-terminal portion of the protein. Dev Dyn 235: 967-977

Wang Z, Bosveld F, Bellaiche Y (2018) Tricellular junction proteins promote disentanglement of daughter and neighbour cells during epithelial cytokinesis. J Cell Sci

Wei SY, Escudero LM, Yu F, Chang LH, Chen LY, Ho YH, Lin CM, Chou CS, Chia W, Modolell J, Hsu JC (2005) Echinoid is a component of adherens junctions that cooperates with DE-Cadherin to mediate cell adhesion. Dev Cell 8: 493-504

Wei X, Malicki J (2002a) nagie oko, encoding a MAGUK-family protein, is essential for cellular patterning of the retina. Nat Genet 31: 150-7

Wei X, Malicki J (2002b) nagie oko, encoding a MAGUK-family protein, is essential for cellular patterning of the retina. Nature Genetics 31: 150-157

Westerfield M (2000) The zebrafish book. A guide for the laboratory use of zebrafish (Danio rerio). Univ. of Oregon Press, Eugene

Zhang L, Kendrick C, Julich D, Holley SA (2008) Cell cycle progression is required for zebrafish somite morphogenesis but not segmentation clock function. Development 135: 2065-2070

Zou J, Wen Y, Yang X, Wei X (2013) Spatial-temporal expressions of Crumbs and Nagie oko and their interdependence in zebrafish central nervous system during early development. International journal of developmental neuroscience 31: 770-782.